Interfacial Energy of Diffuse Phase Boundaries in the Generalized Broken-Bond Approach

B. SONDEREGGER and E. KOZESCHNIK

In the present article, the interfacial energy of coherent, planar phase boundaries is treated theoretically in the framework of the generalized *n* nearest-neighbor broken-bond (NNBB) approach, taking into account that a certain degree of mixing of atoms can occur between the two phases across the phase boundary. This mixing introduces additional entropic contributions to the planar sharp interfacial energy. It is shown that, in this case, the dilute interfacial energy is lower than the energy of the corresponding sharp interface. For the special case of regular solutions, an analytical approximation is developed, which is expressed in relation to the corresponding sharp interface solution. It is shown that the present general broken-bond (GBB) model represents a simple and computationally efficient method for determining diffuse interface energies, particularly in multicomponent systems, where general (*e.g.*, CALPHAD type) thermodynamic data are available.

DOI: 10.1007/s11661-010-0370-8

I. INTRODUCTION

INTERPHASE boundary energies play a key role for the prediction of the microstructure evolution in multiphase materials, particularly for evaluation of nucleation and coarsening rates of precipitates. Efficient modeling approaches for application in multicomponent microstructure evolution simulations demand concepts that, on the one hand, can handle a broad range of compositions and provide reasonably accurate predictions for the interfacial energy and, on the other hand, consume only minimal computational resources. In the present article, we particularly focus on the second aspect, computational time, with the goal of using the present model in a continuums framework for precipitation kinetics simulation.

In literature, a number of methods have been proposed for calculation of interphase boundary energies, with different complexity and varying computational effort. One of the best known classical treatments goes back to the works of Becker[1] and Turnbull,[2] who introduced the nearest-neighbor broken-bond (NNBB) model. In the original treatment, the interphase separating the two crystals is infinitely small, an approximation only valid for sufficiently low temperatures. Later, a number of authors improved the original NNBB model with respect to interface orientation and entropic contributions to the energy at higher temperatures, which are leading to certain concentration profiles at the interface (a more detailed discussion of these models is given in Reference 3). The most comprehensive work on the topic was presented in an article of Lee and Aaronson,[4] who provide temperature-dependent interfacial energies for binary regular solution systems and obtain their results *via* numerical free energy minimization. However, their work remains incomplete due to systematic under-representation of longer distance atomic bonds.[3] This situation motivated the authors to re-evaluate the NNBB model considering arbitrary bond lengths and create a general broken-bond (GBB) model for multicomponent systems. One result, restricting on the case of sharp interface profiles, has been published recently.[3]

Most works within the NNBB framework treat the solid phase as an arrangement of single atoms. Cahn and Hilliard[5] translated this lattice-based description of interfaces into a continuums-mechanical view. This approach simplified the mathematical treatment especially for high temperatures with broad concentration profiles, and later became a starting point for the well-known phase field model. In this model, the interphase boundary is treated in terms of the spatial transition from one phase to another, described by a continuous order parameter.[6] The free energy of the thermodynamic system, as well as the interfacial properties, is then described in terms of this parameter, which usually ranges from zero to one. The part of the energy stemming from the interface is commonly denoted as the gradient energy term. In this type of diffuse interface approach, the actual value of the interfacial energy and the thickness of the interface are evaluated by minimizing the total energy of the system containing the interface.

The cluster variation method (CVM), initially aimed at determining alloy phase diagrams as well as many topics related to phase transitions, was originally based on a rigid lattice approximation.[7,8] This concept was later advanced to include continuous atomic

B. SONDEREGGER, Assistant Professor, is with the Institute for Materials Science and Welding, Graz University of Technology, 8010 Graz, Austria. Contact e-mail: bernhard.sonderegger@tugraz.at E. KOZESCHNIK, Professor, is with the Christian Doppler Laboratory for Early Stages of Precipitation, Institute of Materials Science and Technology, Vienna University of Technology, 1040 Vienna, Austria.
Manuscript submitted June 27, 2009.
Article published online July 20, 2010

displacements due to thermal lattice vibration and local lattice distortions.[9,10] Asta[11,12] studied interphase boundary energies using a tetrahedron-octahedron approximation of the CVM including first- and second-nearest-neighbor interactions. Systematic variations of atom types within the lattice finally reproduce concentration profiles with the lowest energy at a specific temperature. While being considered as a profound and rigorous model, CVM is rather demanding in terms of computational effort.

Recently, the cluster/site approximation (CSA) has been applied to the calculation of coherent interface boundaries[13] at elevated temperatures. Compared to CVM, CSA is less computationally extensive and has been shown to produce good results on real binary alloys, even showing the potential for the application in complex multicomponent materials. Similar to CVM, the interfacial energy is computed *via* numerical free energy minimization, giving the concentration profile as an additional result.

When comparing the individual approaches, the original NNBB concept[1,2] and, recently, the GBB model[3] demand the least computational power, since the interfacial energy (IE) can be expressed as a single, explicit equation. Still these approaches are restricted to sharp interfaces at 0 K, NNBB in binary alloys, and GBB in multicomponent systems. Following the argumentation of Cao *et al.*,[13] CVM[11] can be considered as a benchmark in terms of accuracy, followed by CSA,[13] and finally the thick interface NNBB approach of Lee and Aaronson.[4]

Since the recent attempt to improve NNBB toward GBB without increasing the computational effort has been successful, the next step taken here is to advance the GBB concept from sharp to diffuse interfaces, thereby taking into account the entropic effects at the interface at elevated temperatures. In the course of this process, the sharp interface changes to an interface defined by a concentration gradient across a finite width of the phase boundary. In the general case of the GBB concept for diffuse interfaces, the IE is computed by minimizing the systems Gibbs free energy. In regular solution systems, the result can be expressed by explicit equations. It is shown that both numerical and analytic approaches produce results of good accuracy, even when compared to CSA and CVM.

The main advantages of the GBB concept developed here can be summarized as (1) being numerically inexpensive (especially for systems behaving thermodynamically similar to regular solutions); (2) providing estimates of good accuracy; and (3) using CALPHAD type databases as input data, which are nowadays available for a wide range of multicomponent systems. Particularly, the third aspect proves to be convenient, since precipitation kinetic simulations commonly take advantage of Gibbs free energies and solution enthalpies provided by these databases, and the GBB concept can then be applied straightforwardly without the use of any additional data.

The basic concepts behind the model are briefly reviewed in Section II, followed by a discussion on the model accuracy in regular solutions and real alloys.

II. GENERALIZED *n* NNBB MODEL

Consider two phases I and II, separated by a planar, sharp interface. According to the NNBB model,[1] the interfacial energy can be calculated with respect to the difference of all accumulated bond energies in a system containing an interface, compared to the accumulated bond energies of the same amount of atoms in separated (equilibrium) phases. Originally, only the bonds between nearest-neighbor atoms have been accounted for. Later, the interfacial energy γ_0 of a planar, sharp phase boundary has been expressed in terms of the solution enthalpy ΔE_{sol} as[2]

$$\gamma_0 = \frac{n_S \cdot z_S}{N \cdot z_L} \cdot \Delta E_{\text{sol}} \qquad [1]$$

where N is the Avogadro constant, n_S is the number of atoms per unit area of interface, z_L is the coordination number, and z_s is the number of nearest neighbor broken bonds. It is interesting to note that the first term in Eq. [1] contains only structural quantities related to the type of crystal lattice, whereas the enthalpy of solution represents a purely thermodynamic quantity. Energy contributions from misfit strains in the interface are neglected in this approach.

In Reference 3, the original NNBB approach was generalized to multicomponent systems and to *n*-nearest neighbor interactions. This task was achieved by introducing and evaluating effective quantities $z_{S,\text{eff}}$ and $z_{L,\text{eff}}$. These quantities were evaluated for selected discrete orientations of the interfaces, as well as the average interfacial energy integrated over all possible interface orientations. A mean structural factor of $z_{S,\text{eff}}/z_{L,\text{eff}} = 0.328$ was obtained for the body-centered-cubic (bcc) structure and $z_{S,\text{eff}}/z_{L,\text{eff}} = 0.329$ for the face-centered-cubic (fcc) structure, compared to values of 0.5 and 0.3 in the NNBB approach.

When going from planar to curved interfaces, the process of accumulating *all* bond energy terms turned out to be rather involved. In an approximation, which was introduced in the appendix of Reference 3, and which is used further in the present work, the individual atoms are replaced by infinitesimal volume elements with constant density (number of atoms per volume element). The total energies can then be obtained by integration of the density functions. It has been necessary, however, to introduce a minimum bond length, accounting for the fact that atoms cannot approach each other arbitrarily close. This concept has made it possible to apply the GBB model to more complex geometries such as, *e.g.*, interfaces of spherical precipitates.[14] Also, in Reference 14, the numerical value of the minimum bond length (lower integration limit) has been evaluated with $r_k = 0.3r_1$, with r_1 being the nearest-neighbor distance. This result will also be used in this article.

III. DIFFUSE INTERFACE MODEL

Figure 1 presents a sketch of concentration profiles across interfaces as assumed in the present model. The concentration profile of elements across the interface is

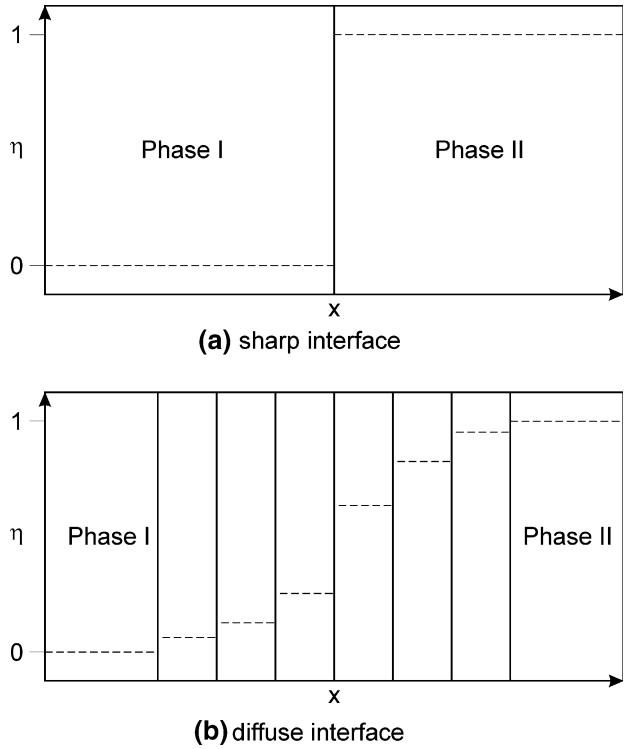

Fig. 1—Schematic concentration profiles of sharp and diffuse interfaces.

parameterized by the variable η, which is considered to be discrete, here, in contrast to the continuous order parameter of the phase-field approach. The diffuse interface is represented by a given number of layers with certain thickness and concentration. Each layer represents a lattice plain or a semi-infinite bulk volume.

In analogy to the sharp interface treatment, the total free energy of the diffuse interface can be calculated by summing up the interaction energies of all volume elements with volume elements of different composition. However, it is important to recognize that, in contrast to the sharp interface treatment, entropy contributions in the individual interface layers must now be taken into account. These are omitted in the conventional NNBB and GBB approaches because the interface is assumed to be infinitely small.

In evaluating the energy of diffuse interfaces, it is necessary to consider two types of energy contributions: the bulk-free energies of the individual layers and the interaction energies between the layers. In order to define the free energy contribution of each layer, one has to keep in mind that the interfacial energy is defined as the difference in energy of the entire system containing an interface and the energy of two separate homogeneous reference systems without interfaces. Thus, the energy contribution of each layer is given by its free energy reduced by the energy of the same amount of matter being either pure phase I or II, respectively. According to Figure 1(b), for calculation of the interfacial energies, one has to consider (1) the interaction energy of bulk phases I and II, (2) the interaction energy of each interface layer with bulk phase I, (3) the interaction energy of each interface layer with bulk phase II, and (4) the interaction energy of each interface layer with each other interface layer.

The interfacial energy γ of the system with a diffuse interface is finally evaluated as the sum of all interactions (1) through (4) plus the bulk-free energies of all layers minus the bulk-free energy of the same amount of matter of separate (equilibrium) phases. Accordingly, for the diffuse interfacial energy γ, the following symbolic equation holds:

$$\gamma = \gamma_{\mathrm{I,II}} + \sum_{q=1}^{n} \gamma_{\mathrm{I},q} + \sum_{p=1}^{n} \gamma_{\mathrm{II},p} + \sum_{p=1}^{n-1} \sum_{q=p+1}^{n} \gamma_{pq} + \sum_{p=1}^{n} \gamma_{G,p} \quad [2]$$

where n represents the number of layers and p and q are the corresponding layer indices. In the present case, we consider a closed system under constant pressure. Therefore, in the following treatment, we use the Gibbs energy to represent the free energy of the system.

Each single interaction energy is now treated analogously to the energy of a sharp interface. Accordingly, the energy contains structural and compositional contributions. Since z_L, n_s, and N do not depend on the interface properties, all contributions can be expressed by effective values of z_S and ΔE_{sol}, respectively. The interaction energies can then be expressed by

$$\gamma = \gamma_0 \cdot \frac{z_S}{z_{S,0}} \cdot \frac{\Delta E_{\mathrm{sol}}}{\Delta E_{\mathrm{sol},0}} = \gamma_0 \cdot \alpha(z_S) \cdot \beta(\Delta E_{\mathrm{sol}}) \quad [3]$$

where γ_0, $z_{S,0}$, and $\Delta E_{\mathrm{sol},0}$ represent the corresponding properties of the sharp interface. In this general expression for the interfacial energy of a diffuse interface, the factor α takes into account the spatial arrangement of the system and β accounts for the influence of the chemical composition of the interacting volumes.

In order to develop an expression for α, consider first the generic case of two neighboring layers with given thickness (which is infinite for the limiting layers of reference phases I and II). This case will be generalized later to include a gap between the two layers, making it suitable for the general treatment of cases (1) through (4). Let the two layers be separated by a sharp interface. The left layer contains volume elements denoted as dV_{I} and the right layer dV_{II}. The potential function between two volume elements is denoted as $f(r/r_1)$, with r being the distance between the volume elements. dV_{I} has the normal distance a to the interface and $\mathrm{d}V_{\mathrm{II}}$ the normal distance b. The term h denotes the cathetus in the triangle sketched in Figure 2.

With this convention, a weight d_b for the bond energy between dV_{I} and dV_{II} can be introduced:

$$d_b = n_V dV_{\mathrm{I}} \cdot n_{\mathrm{V}} dV_{\mathrm{II}} \cdot f(r/r_1) \quad [4]$$

with n_V being the number of atoms per volume. Due to the planar symmetry of the system, dV_{I} can be replaced by $A \cdot da$, with A being the size of the interfacial area. The d_b can then be immediately transformed to dz_S, the number of bonds per atom at the interface.

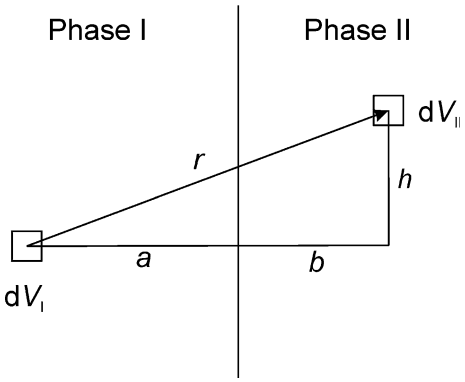

Fig. 2—Volume elements relative to a sharp interface.

This transformation has also been used in References 3 and 14. After integration, z_S can be directly used in the calculation of the interfacial energy, Eq. [1], with

$$dz_S = n_V^{4/3} \cdot f(r/r_1) \cdot da \cdot dV_{\mathrm{II}} \qquad [5]$$

The term dV_{II} can now be replaced by the corresponding infinitesimal variables db and dh, yielding

$$dz_S = n_V^{4/3} \cdot f(r/r_1) \cdot 2h\pi \cdot da \cdot db \cdot dh \qquad [6]$$

This equation can be integrated after inserting a specific weighting function f. Analogously to References 3 and 14, we apply a Lennard–Jones potential function of type r^{-6}, which leads to

$$f(r/r_1) = (r/r_1)^{-6} = \left[(a+b)^2 + h^2\right]^{-3} \cdot r_1^6 \qquad [7]$$

and

$$dz_S = 2\pi \cdot n_V^{4/3} \cdot r_1^6 \cdot \left[(a+b)^2 + h^2\right]^{-3} \cdot h \cdot da \cdot db \cdot dh \qquad [8]$$

This equation can be integrated with respect to h. In order to capture all bonds in plane b, h is integrated from $-\infty$ to ∞. The result given in Eq. [9] represents the number of bonds between two parallel planes located in the distance $a + b$ with

$$dz_S = \frac{\pi}{2} \cdot n_V^{4/3} \cdot r_1^6 \cdot (a+b+r_k)^{-4} \cdot da \cdot db \qquad [9]$$

This intermediate result is the basis for all further calculations in this article. In the case of two semi-infinite layers, which represent two phases I and II, a and b are integrated from 0 to ∞, respectively, yielding

$$z_{S,0} = \frac{\pi}{2} \cdot n_V^{4/3} \cdot r_1^6 \cdot \int_{a=0}^{\infty} \int_{b=0}^{\infty} (a+b+r_k)^{-4} \cdot da \cdot db \qquad [10]$$

with the solution

$$z_{S,0} = \frac{\pi}{12} \cdot n_V^{4/3} \cdot r_1^6 \cdot r_k^{-2} \qquad [11]$$

Equation [11] represents the energy of a sharp interface; consequently, z_S is denoted as $z_{S,0}$ in this case. Inserting Eq. [11] into Eq. [1] reproduces exactly the mean energy of a sharp, planar interface, if the GBB values for z_L and r_k are used ($z_{L,\mathrm{bcc}} = 12.234$, $z_{L,\mathrm{fcc}} = 14.442$, and $r_k = 0.3r_1$; References 3 and 14).

Using Eq. [10], the more general case of interactions with a gap of size c between the layers can be written as

$$z_S = \frac{\pi}{2} \cdot n_V^{4/3} \cdot r_1^6 \cdot \int_{a=\frac{c}{2}}^{a_0+\frac{c}{2}} \int_{b=\frac{c}{2}}^{b_0+\frac{c}{2}} (a+b+r_k)^{-4} \cdot da \cdot db \qquad [12]$$

where a_0 and b_0 represent the layer thickness. Integration of Eq. [12] leads to the following solutions for α:

$$\alpha_{pq} = r_k^2 \cdot \Big[(a_0+b_0+c+r_k)^{-2} + (r_k+c)^{-2} - (a_0+c+r_k)^{-2} - (b_0+c+r_k)^{-2}\Big] \qquad [13a]$$

for the interaction of layer p with layer q,

$$\alpha_{\mathrm{I},q} = r_k^2 \cdot \Big[(r_k+c)^{-2} - (b_0+c+r_k)^{-2}\Big] \qquad [13b]$$

for the interaction of layer q with phase I,

$$\alpha_{\mathrm{II},p} = r_k^2 \cdot \Big[(r_k+c)^{-2} - (a_0+c+r_k)^{-2}\Big] \qquad [13c]$$

for the interaction of layer p with phase II, and finally

$$\alpha_{\mathrm{I,II}}(c) = r_k^2 \cdot (r_k+c)^{-2} \qquad [13d]$$

for the interaction of phase I with phase II.

We can now calculate the factor β from Eq. [3], accounting for the chemical compositions of the layers. In this work, we constrict ourselves to the case where the chemical composition can be parameterized by only one parameter, η. This simplification excludes individual segregations of elements at the phase boundary, and it implies that all concentration profiles have the same shape. However, this assumption allows us to obtain an analytical solution to the problem that is exact for a regular solution two-component system. In higher-order multicomponent systems, the model delivers an upper-boundary estimate of the interfacial energy.

Let x_i^p and x_j^q be the composition of layers p and q, with i and j denoting the components. The quantities x_i^{I} and x_j^{II} are the compositions of phases I and II. As introduced by Becker[1] for a two-component system and generalized to multicomponent systems in the appendix of Reference 3, the solution enthalpy can be calculated by accumulating all bond energies, yielding

$$\Delta E_{\mathrm{sol}} = N \cdot z_L \cdot \varepsilon_0 \qquad [14]$$

with

$$\varepsilon_0 = \sum_{i,j} \varepsilon_{ij} \left[x_i^p x_j^q - \frac{1}{2}\left(x_i^p x_j^p + x_i^q x_j^q\right)\right] \qquad [15]$$

in the case of the interaction between two layers. For the interaction with one of the phases I and II, x^p and x^q have to be replaced by x^{I} and x^{II}, respectively. The term ε_{ij} denotes the bond energy between two

neighboring atoms of types i and j. The compositions of layers p and q are now parameterized by η_p and η_q.

$$x_i^p = \eta_p x_i^{\mathrm{I}} + (1-\eta_p) x_i^{\mathrm{II}} \quad [16a]$$

$$x_j^q = \eta_q x_j^{\mathrm{I}} + (1-\eta_q) x_j^{\mathrm{II}} \quad [16b]$$

This parameterization leads to

$$\beta_{pq} = (\eta_p - \eta_q)^2 \quad [17a]$$

$$\beta_{\mathrm{I}q} = \eta_q^2 \quad [17b]$$

$$\beta_{\mathrm{II}p} = (1-\eta_p)^2 \quad [17c]$$

Finally, the last term in Eq. [2], representing the difference in volume free energy of each interface segment, is evaluated.

Assume that we have two blocks of phases I and II with compositions x_i^{I} and x_i^{II}, with no contact to each other, and the molar Gibbs energies g_{I} and g_{II}. When brought into contact, the atoms at the interface will start to intermix with each other to some degree and develop a diffuse interface with thickness t. Each layer p can be characterized by a composition x_i^p, with the molar Gibbs energy g_p. An excess Gibbs energy of the interfacial volume can then be defined as the Gibbs energy of the diffuse interface volume, reduced by the Gibbs energy of the corresponding separate phases I and II in the unmixed state. If we assume that half of the interface thickness stems from phase I and the other half from phase II, within an interfacial region of area A with thickness t, the excess Gibbs energy is given as

$$\Delta G = \left(\sum_{p=1}^{n} g_p(\eta_p) \cdot a_{0,p} \cdot A/\Omega \right) - g_{\mathrm{I}} \cdot A \cdot \frac{t}{2}/\Omega - g_{\mathrm{II}} \cdot A \cdot \frac{t}{2}/\Omega \quad [18]$$

where Ω is the molar volume and $a_{0,p}$ is the thickness of layer p. Alternatively, this energy can be normalized to a unit area of interface, thus converting ΔG to $\gamma_{G,p}$. Each layer p then contributes to the interfacial energy with

$$\gamma_{G,p} = \left[g_p(\eta_p) - \frac{g_{\mathrm{I}} + g_{\mathrm{II}}}{2} \right] \cdot a_{0,p}/\Omega \quad [19]$$

With Eqs. [2], [13], [17], and [19], all ingredients for calculation of the energy of a diffuse interface are at hand and the interfacial energy corresponding to arbitrary interfacial composition profiles can be evaluated. The equilibrium profile and the actual interfacial energy value can be obtained after minimization of the total free energy of the system using standard numerical procedures.

It is important to note that the present model does not rely on a specific thermodynamic solution model such as, for instance, the well-known regular solution. The main input parameters are the energy of the sharp interface γ_0, the chemical composition of phases I and II, and the corresponding molar Gibbs free energies. The equations shown above can thus be applied to any system where thermodynamic data are available, for instance, in the form of general multicomponent CALPHAD-type databases.[15]

IV. REGULAR SOLUTION APPROXIMATION

In specific situations, it might be of interest if the equations derived in the previous section can be simplified to allow for an approximate explicit analytical evaluation of the interfacial energy instead of having to perform numerical energy minimization. Indeed, for regular solutions, it is possible to derive an approximation, which can be expressed in the form of a single, explicit equation. This approximation is beneficial when calculation time is costly, as it is the case in, *e.g.*, complex precipitation kinetics simulations. Furthermore, some benchmark literature data are available for this case, derived by the NNBB model,[4] CSA,[13] and CVM,[11] respectively. In Sections IV and V, the corresponding analytical expressions are derived and verified against the numerical solution of the present approach and the literature data.

The following analytic expressions are based on a simplified model, which only considers two interfacial layers. The derivation is restricted to a two-component system. Multicomponent systems can be treated analogously and lead to the same result, if the individual concentration profiles are assumed to have the same general shape. The composition of phase I is given by x_{I}, the composition of layer 1 by x. Due to the symmetry of the regular solution potential function and the mass balance, the compositions of phase II and layer 2 are given as

$$x_{\mathrm{II}} = 1 - x_{\mathrm{I}} \quad [20]$$

$$x_2 = 1 - x$$

If x_{I} is fixed at the beginning of the calculations (by, *e.g.*, assuming equilibrium between the two phases), x is the only parameter left for defining the concentration profile and, thus, the interface energy. The task, now, is to minimize the interfacial energy with respect to x and reinsert the result in the interfacial energy equations.

The interfacial energy consists of an interaction part and a volumetric part. Let us first consider the volumetric part. In a regular solution, the molar Gibbs energy is given by

$$g = N \cdot \frac{z_L}{2} \cdot \left[\varepsilon_{11} x^2 + 2\varepsilon_{12} x(1-x) + \varepsilon_{22}(1-x)^2 \right] + \mathrm{R}T \cdot [x \cdot \ln x + (1-x) \cdot \ln(1-x)] \quad [21]$$

with R being the gas constant; T the temperature; and ε_{11}, ε_{12}, and ε_{22} the interaction energies of neighboring

atoms of types 1 and 2. In our case, the effective Gibbs energy of one layer is given by the energy difference between this layer and a corresponding bulk phase. This effective energy remains equal, if some constant factor is subtracted from both contributions.

This observation is used for simplifying the expression for the Gibbs energy, which leads to a modified molar Gibbs energy g^* reading

$$g^* = N{\cdot}z_L{\cdot}\varepsilon^*{\cdot}x(1-x) + \mathrm{R}T{\cdot}[x{\cdot}\ln x + (1-x){\cdot}\ln(1-x)] \quad [22]$$

where

$$\varepsilon^* = \varepsilon_{12} - \varepsilon_{11}/2 - \varepsilon_{22}/2 \quad [23]$$

The term ε^* is also applied for calculation of the solution enthalpy. The enthalpy term in Eq. [22] can be expressed by the solution enthalpy at 0 K, which is

$$\Delta E_{\mathrm{sol,0K}} = N{\cdot}z_L{\cdot}\varepsilon^* \quad [24]$$

The free energy of the system then reads

$$g^* = \Delta E_{\mathrm{sol,0K}}{\cdot}x(1-x) + \mathrm{R}T{\cdot}[x{\cdot}\ln x + (1-x){\cdot}\ln(1-x)] \quad [25]$$

In order to compare our results with literature data, all temperatures are normalized with respect to the regular solution critical temperature T_C. The value of T_C is the highest possible solution temperature, which is observed at a system composition of $x_A = x_B = 0.5$, and T_C is defined as

$$T_C = \Delta E_{\mathrm{sol,0K}}/2R \quad [26]$$

When setting the thickness of all layers d constant and identical to the lattice plane distance, one arrives at the expression for the volumetric contribution to the interfacial energy with

$$\gamma_G = \frac{2RZd}{a^3N}{\cdot}\{2T_C{\cdot}[(x-x^2)-(x_\mathrm{I}-x_\mathrm{I}^2)] + T{\cdot}[x{\cdot}\ln x + (1-x){\cdot}\ln(1-x) - x_\mathrm{I}{\cdot}\ln x_\mathrm{I} - (1-x_\mathrm{I}){\cdot}\ln(1-x_\mathrm{I})]\} \quad [27]$$

where a is the unit cell size and Z is the number of atoms per unit cell. Analogously to the general treatment, we express γ_G in terms of the sharp interface energy, γ_0, *via* $\gamma_G = f_G{\cdot}\gamma_0$. When expressing γ_0 in terms of Z, a, and T_C as

$$\gamma_0 = \frac{z_S}{z_L}{\cdot}\frac{Z^{2/3}}{a^2N}{\cdot}2\mathrm{R}T_C \quad [28]$$

one arrives at

$$f_G = Z^{1/3}\frac{d}{a}{\cdot}\frac{z_L}{z_S}{\cdot}\left\{2[(x-x^2)-(x_\mathrm{I}-x_\mathrm{I}^2)] + \frac{T}{T_C}[x{\cdot}\ln x + (1-x){\cdot}\ln(1-x) - x_\mathrm{I}{\cdot}\ln x_\mathrm{I} - (1-x_\mathrm{I}){\cdot}\ln(1-x_\mathrm{I})]\right\} \quad [29]$$

The contribution of interaction energies are calculated in analogy to Eq. [3], which leads to

$$f_{\mathrm{inter}} = \alpha_{\mathrm{I,II}}(1-2x_\mathrm{I})^2 + 2\alpha_{\mathrm{I},1}(x-x_\mathrm{I})^2 + 2\alpha_{\mathrm{I},2}(1-x-x_\mathrm{I})^2 + \alpha_{1,2}(1-2x)^2 \quad [30]$$

In order to find the layer concentration x, the sum of contributions f_G and f_{inter} has to be minimized with respect to x, leading to an implicit equation for x as

$$2{\cdot}(1-2x) + 4Z^{-1/3}\frac{z_S}{z_L}{\cdot}\frac{a}{d}[\alpha_{\mathrm{I},1}(x-x_\mathrm{I}) - \alpha_{\mathrm{I},2}(1-x-x_\mathrm{I}) - \alpha_{1,2}(1-2x)] - \frac{T}{T_C}\ln\left(\frac{1}{x}-1\right) = 0 \quad [31]$$

Assuming that the target concentration x is reasonably close to x_I, which is the case at low and medium temperatures, delivers the final explicit expression reading

$$x = \left\{1 + \exp\left[K\frac{T_C}{T}{\cdot}(1-2x_\mathrm{I})\right]\right\}^{-1} \quad [32]$$

where K contains the influence of the interface and crystal structure with

$$K = 2 - 4Z^{-1/3}\frac{z_S}{z_L}{\cdot}\frac{a}{d}[\alpha_{\mathrm{I},2} + \alpha_{1,2}] \quad [33]$$

With Eqs. [28] through [30], [32], and [33], the approximate dilute interface energy becomes a function of temperature, crystal structure, and interface orientation only, and can be evaluated straightforwardly. Table I provides the corresponding input parameters for some interface orientations.

V. RESULTS AND DISCUSSION

In this section, the GBB model is compared against the literature data of CVM and CSA calculations and experimental data derived from precipitate evolutions.

The ideal benchmark for comparing the models is the binary regular solution system, since it is simple enough to exclude side effects originating from different thermodynamic data. *Via* defining a critical interaction temperature T_C, all interaction energies are well defined and also the Gibbs free energy can be calculated

Table I. Factors for Specific Interfaces in Fcc and Bcc Lattices; z_S/z_L Taken from Reference 3

	Fcc			Bcc		
	[100]	[110]	[111]	[100]	[110]	[111]
$\alpha_{\mathrm{I,II}}$	0.0533	0.0887	0.0425	0.0533	0.0306	0.1169
$\alpha_{\mathrm{I},1}$	0.8594	0.7893	0.8831	0.8594	0.9113	0.7403
$\alpha_{\mathrm{I},2}$	0.0874	0.1220	0.0744	0.0874	0.0581	0.1428
$\alpha_{1,2}$	0.7720	0.6673	0.8087	0.7720	0.8532	0.5975
d/a	1/2	$1/(2\sqrt{2})$	$1/\sqrt{3}$	1/2	$1/\sqrt{2}$	$1/(2\sqrt{3})$
z_S/z_L	0.3105	0.3271	0.2871	0.3332	0.2905	0.3351
Z	4			2		
K	0.6552	0.1599	0.8935	0.1818	0.8114	–0.7282

straightforwardly. In other systems representing a real material, interaction- and many-body-energies (CVM/CSA) and CALPHAD-type thermodynamic databases (GBB/NNBB) usually stem from different sources. In order to exclude these complications, the discussion will restrict on binary regular solutions.

For this system, Lee and Aaronson[4] provide data for fcc lattices and (100) interface orientations derived by the NNBB model; Cao *et al.* calculated the same data with CSA[13] and Asta with CVM.[11] Figure 3 shows the result of each of the models, including the GBB model and the analytical approximation of GBB. For convenience, the interfacial energy was normalized with respect to $k_B T_C/a^2$, and the temperature was normalized with respect to T_C. Since the cluster variation method is the physically most profound model, it acts as a benchmark.

From Figure 3, we observe that all models show similar characteristics, having the maximum interfacial energy at 0 K, a constant high value up to approximately 0.2 T_C, followed by a smooth decline, and finally reaching zero at T_C. Generally, the NNBB model predicts slightly lower interfacial energies than the other models. With the introduction of GBB instead of NNBB, the characteristics of the interfacial energy approach the benchmark of CVM very closely. Furthermore, GBB coincides virtually exactly with CSA at low temperatures (at these temperatures, no CVM data are available). Since the interface is considered to be ideally sharp at 0 K, this agreement is solely due to the good estimation of the structural factor z_S/z_L of 0.3105 (Reference 3 and Table I). Also, at elevated temperatures, the differences between CSA, GBB, and CVM are only minor, with GBB slightly closer to the CVM benchmark than CSA. The analytical approximation of GBB is in very good agreement with the benchmark as well; the deviations are minor.

In order to test the GBB model on real systems, we have chosen a system where accurate thermodynamic data are available, as well as carefully obtained experimental information. Generally, IEs can be measured by precipitate coarsening and nucleation experiments; ideally both measurement routines are carried out independently on the same system. One of the best-examined systems, in this respect, is the γ/γ' system in Ni-Al binary alloys. For this, a thermodynamic database (Ni_data_v30[16]) is available to feed the NNBB and GBB model. Moreover, in the last decades, a number of scientific groups have dealt with the task of analyzing the coarsening kinetics of γ' precipitates. Frequently, a seminal article of Ardell[17] is used as a source of carefully assessed experimental data, which has been interpreted with coarsening models of increasing sophistication, *e.g.*, by Chellman and Ardell,[18] Yang and Nash,[19] Ardell,[20] and Li *et al.*[21] In this work, Ardell measured coarsening rates and solute concentrations of Al in the matrix independently, which eliminated the diffusion coefficients in the rate equations and increased the accuracy of the analysis significantly. Ardell assumed the original LSW theory to be valid, an approach that was improved later toward volume-corrected LSW theories (review by Voorhees[22]). These advanced coarsening kinetic treatments were applied by a number of authors to the NiAl systems, such as Chellman and Ardell,[18] Yang and Nash,[19] and Calderon and Voorhees.[23] Ardell[20] re-evaluates his own results and ends up with much lower interfacial energies than initially found. However, Li *et al.*[21] pointed out that the Ni-Al system shows a quite nonideal thermodynamic behavior, which has to be taken into account explicitly. Using the newest thermodynamic data available and re-evaluating Ardell's data, Li *et al.* end up with interfacial energies of 21 to 24 mJ/m^2 at 898 K and 998 K (625 °C and 725 °C). This result is going to be the experimental benchmark in the following.

Wagner *et al.*[24] report slightly smaller IEs of 16 mJ/m^2 obtained by nucleation experiments. This decrease of IEs due to the strong curvature of the

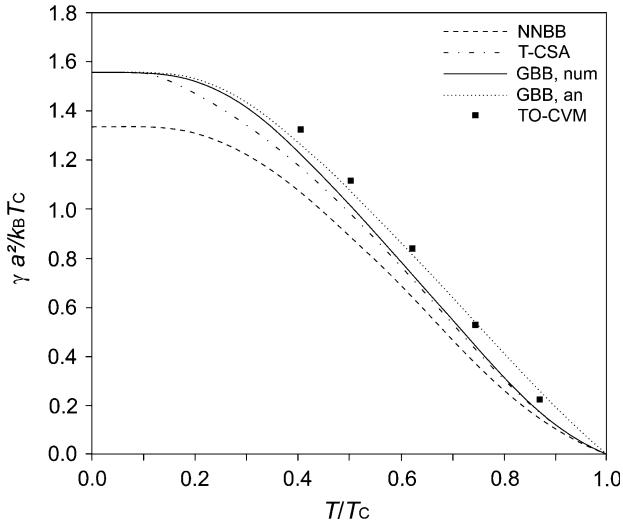

Fig. 3—Interfacial energy of an (100) interface in fcc systems. NNBB model (Ref. 4), T-CSA,[13] TO-CVM,[11] and analytical (GBB, an) and numerical GBB (GBB, num) approach.

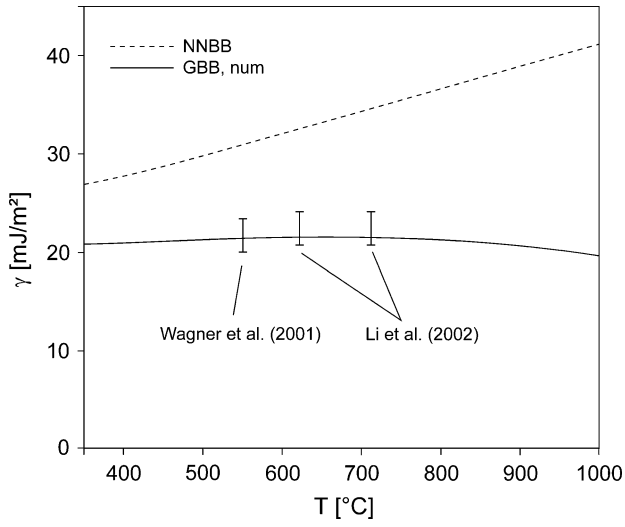

Fig. 4—Energy of γ/γ' interfaces in Ni-Al systems. Calculated values for NNBB and GBB model, experimental evaluations from Li *et al.*[21] and Wagner *et al.*[24]

nucleus interface has been depicted theoretically by Kashchiev.[25] A recent estimation of this effect by Sonderegger and Kozeschnik[14] suggests a multiplicative factor of 0.7 to 0.8 for typical nuclei. Taking Wagner's results and considering the change of IEs due to these size effects, one ends up with an energy of 20 to 23 mJ/m^2 for the planar interfaces, which is in excellent agreement with the coarsening data of Li *et al.*

Figure 4 summarizes these experimental values in comparison with the predicted results obtained by the NNBB and the GBB model. Whereas the original NNBB generally overestimates the interfacial energies, the results of the GBB coincide well with the experimental findings.

VI. SUMMARY

In the present work, the generalized *n* NNBB concept is applied to the calculation of the energy of a diffuse coherent planar phase boundary, which is represented by individual atomic layers. It is shown that the interfacial energy can be evaluated by accumulating all energetic interactions between the individual layers and the bounding bulk volumes. The energy of each layer is expressed in terms of the Gibbs free energy, thus accounting for the entropic contributions to the interfacial energy of diffuse phase boundaries. The interface constitution with lowest free energy is evaluated by minimization of the total free energy of the system.

Provided that temperature- and composition-dependent molar Gibbs energies are available, the energy and the concentration profile across a diffuse interface can be conveniently evaluated for any multicomponent alloy. It is assumed, however, that the concentration profiles of all elements are identical. Comparisons with experimental data of γ' precipitates in Ni-Al systems underline the potential of the new method.

Finally, an explicit analytical expression is derived for the case of a regular solution. It is shown that both the numerical and analytical expressions proof well against literature data while keeping computational effort minimal.

ACKNOWLEDGMENTS

Financial support by the Österreichische Forschungsförderungsgesellschaft mbH, the Province of Styria, the Steirische Wirtschaftsförderungsgesellschaft mbH, and the Municipality of Leoben within research activities of the Materials Center Leoben Forschung GmbH under the frame of the Austrian Kplus Competence Center Programme is gratefully acknowledged.

REFERENCES

1. R. Becker: *Ann. Phys.*, 1938, vol. 32, pp. 128–40.
2. D. Turnbull: *Impurities and Imperfections*, ASM, Metals Park, OH, 1955, pp. 121–43.
3. B. Sonderegger and E. Kozeschnik: *Metall. Mater. Trans. A*, 2009, vol. 40A, pp. 499–510.
4. Y.W. Lee and H.I. Aaronson: *Acta Metall.*, 1980, vol. 28, pp. 539–48.
5. L.W. Cahn and J.E. Hilliard: *J. Chem. Phys.*, 1958, vol. 28, pp. 258–67.
6. I. Steinbach, F. Pezzola, B. Nestler, M. Seesselberg, R. Prieler, G. J. Schmitz, and J.L.L. Rezende: *Physica D*, 1996, vol. 94, pp. 135–47.
7. R. Kikuchi: *Phys. Rev.*, 1951, vol. 81, pp. 988–1003.
8. R. Kikuchi and J.W. Cahn: *Acta Metall.*, 1979, vol. 27, pp. 1337–53.
9. R. Kikuchi and A. Beldjenna: *Physica A*, 1992, vol. 182, pp. 617–34.
10. R. Kikuchi and K. Masudo-Jindo: *CALPHAD*, 2002, vol. 26, pp. 33–54.
11. M.D. Asta: *Theory and Application of the Cluster and Path Probability Methods*, Plenum, New York, NY, 1996, pp. 247–254.
12. M. D. Asta: *Acta Mater.*, 1996, vol. 44, pp. 4131–36.
13. W. Cao, J. Zhu, F. Zhang, W.A. Oates, M. Asta, and Y.A. Chang: *Acta Mater.*, 2006, vol. 54, pp. 377–83.
14. B. Sonderegger and E. Kozeschnik: *Scripta Mater.*, 2009, vol. 60, pp. 635–38.
15. N. Saunders and A.P. Miodownik: *CALPHAD: A Comprehensive Guide*, Pergamon Materials Series, Elsevier, Oxford, United Kingdom, 1998, vol. 1.
16. ThermoTech. Ni-base version 3.0, <http://www.thermotech.co.uk/databases.html>.
17. A.J. Ardell: *Acta Metall.*, 1968, vol. 16, pp. 511–16.
18. D.J. Chellman and A.J. Ardell: *Acta Metall.*, 1974, vol. 22, pp. 577–88.
19. S.C. Yang and P. Nash: *Mater. Sci. Technol.*, 1988, vol. 10, pp. 860–66.
20. A.J. Ardell: *Interf. Sci.*, 1995, vol. 3, pp. 119–25.
21. X. Li, N. Saunders, and A.P. Miodownik: *Metall. Mater. Trans. A*, 2002, vol. 33A, pp. 3367–73.
22. P.W. Voorhees: *J. Stat. Phys.*, 1985, vol. 38, pp. 231–52.
23. H.A. Calderon and P. E. Voorhees: *Acta Metall. Mater.*, 1994, vol. 42, pp. 991–1000.
24. R. Wagner, R. Kampmann, and P.W. Vorhees: in *Phase Transformations in Materials*, G. Kostorz, ed., Wiley-VCH, Weinheim, Germany, 2001, pp. 309–406.
25. D. Kashchiev: *Nucleation: Basic Theory with Applications*, Butterworth-Heinemann, Burlington, MA, 2000, pp. 79–82.